

Abstract. By using images from the HST/WFPC2/ACS archive, we have analyzed the spatial distribution of the AGB and RGB stars along the galactocentric radius of nearby spiral galaxies M 81, NGC 300 and NGC 55. Using color-magnitude diagrams and stellar luminosity functions, we gauge the stellar contents of the surroundings of three galaxies. The red giant population (RGB) identified at large galactocentric radii yields a distance of 3.85 ± 0.08 Mpc for M 81, 2.12 ± 0.10 Mpc for NGC 55, and 2.00 ± 0.13 Mpc for NGC 300, and a mean stellar metallicity of -0.65 , -1.25 , and -0.87 . We find that there are two number density gradients of RGB stars along the radius, which correspond to the thick disk and halo components of the galaxies. We confirm the presence of metallicity gradient of evolved stars at these galaxies, based on the systematic changes of the color distribution of red giant stars. These results imply that thick disk might be a general feature of the spiral galaxies, and endorse a further investigation of the outer stellar edges of nearby spirals, which is critical in constraining the origin and evolution of galaxies.

Key words: Galaxies: individual: M 81, NGC 55 and NGC 300 — galaxies: stellar content — galaxies: photometry — galaxies: structure

A&A manuscript no.
(will be inserted by hand later)

Your thesaurus codes are:
missing; you have not inserted them

Thick disks and halos of spiral galaxies M 81, NGC 55 and NGC 300. *

Tikhonov N.A.^{1,2}, Galazutdinova O.A.^{1,2}, Drozdovsky I.O.^{3,4}

¹ Special Astrophysical Observatory, Russian Academy of Sciences, N.Arkhыз, KChR, 369167, Russia

² Isaac Newton Institute of Chile, SAO Branch, Russia

³ Spitzer Science Center, Caltech, MC 220-6, Pasadena, CA 91107, USA

⁴ Astronomical Institute, St.Petersburg University, 198504, Russia

Received December 2, 2024

1. Introduction

The fossil record of galaxy formation and evolution is imprinted on the spatial distribution, ages and metallicities of galactic stellar populations. The properties of the outer parts of galaxies are very sensitive to both galaxy star formation history and the nature of the intergalactic medium.

The various studies of the nearest spiral galaxies (Milky Way, M31, M33) revealed their similar structure: bulge, thin and thick disks, and halo (van der Marel, 2001; Zocalli et al., 2002; Sarajedini & van Duyne, 2001; Pritchett & van der Bergh, 1988; Belazzini et al., 2003; Guillardre et al., 1998; Brown et al., 2003; Zucker et al., 2004). Aside from the spatial distribution law and kinematics, stars from each of this subsystem share the common star formation history retaining considerable age and chemical information (Vallenary et al., 2000; Prochaska et al., 2000; Chiba & Beers, 2000; Zoccali et al., 2002; Williams, 2002, Sarajedini et al., 2000, Brewer et al., 2003).

The majority of the investigations concentrated predominantly on the central parts of these galaxies, biased towards high surface brightness star forming regions. In recent years, wide-field observations of the nearest spirals have shown that they are substantially more extended than previously thought. The information on the actual origin of these outer regions is scarce, and has been a matter of debates. Today, we know that most of these extended, elusive stellar components are predominantly evolved, but whether this is a true single burst ancient stellar population, with little or no intermediate-age

* Based on observations with the NASA/ESA Hubble Space Telescope, obtained at the Space Telescope Science Institute, which is operated by the Association of Universities for Research in Astronomy, Inc., under NASA contract NAS 5-26555.

component has not yet been established. By ‘population’, we mean here an ensemble of stars that share a coherent history.

Tests of formation scenarios have centered on two extreme viewpoints — (1) the monolithic collapse model for the halo (Eggen et al., 1962) together with internal chemodynamical evolution for the thick disk (e.g. Burkert et al., 1992), and (2) the accretion model for both, the halo (Searle & Zinh, 1978) and the thick disk (Carney et al., 1989; Gilmore, Wyse and Norris 2002). In view of merging Sagittarius dwarf galaxy with Milky Way (Ibata, Gilmore & Irwin 1995), and the predictions of cold dark matter (CDM) cosmological models for hierarchical galaxy formation from large number of mergers, the origin of the thick disk and halo is especially relevant. On other hand, there are evidences for the significant difference between chemical abundance pattern of the Milky Way’s halo stars and the remaining satellite galaxies, indicating of a different evolution history (Brewer & Carner, 2004; Venn et al., 2004).

It is rather easier to separate the spherical bulge and exponential thin disk components based on their distinctive surface brightness profiles (Kent, 1985; Byun & Freeman, 1995; Bagget et al., 1998; Prieto et al., 2001), than the thick disk from halo, due to an extremely low surface brightness of these galaxy components, typically below the 26 mag/□". While some of the resent studies of the outer regions of spiral galaxies was based on the multicolor surface photometry, the successful detection is possible either in the nearest galaxies or in the galaxies with a bright and extended thick disk/halo (e.g. Harris & Harris, 2001). For example, Dalcanton & Bernstein (2002) analyzed the sample of 47 edge-on spiral galaxies and have found a presence of the thick disk in 90% of them, based on the results of multicolor surface photometry. Star number counts are more optimal for studying galactic outskirts due to their extremely low surface brightness and the possibility to eliminate young stars from the thin disk and background objects.

Our goal here is to extend the study of stellar thick disks and halos over a set of spiral galaxies outside the Local group. M 81, NGC 55 and NGC 300 may provide a contrasting environment, and opportunity to examine the stellar populations on larger galactic scales. In particular we address the following two issues: the spatial distribution of different stellar populations in the outskirts of spiral galaxies and the metallicity gradient of these populations. The brief information about the galaxies is given in Table 1. Each of these object has the HST images of several fields, situated in various distances from center. The high spatial resolution of HST allows us to make photometry stars even in dense stellar fields. The availability of images on various galactocentric distances allows us to reconstruct the behavior of stellar density along a galactocentric radius. Since thick disks and halo consists of old stars - red giants and, to a lesser degree, AGB stars - therefore only these stars were in our consideration. The young stellar populations, located at

thin disks of galaxies, have been studied in details (Zickgraf et al., 1990; Georgiev et al., 1992a,b; Pritchet et al., 1987; Kizskurno-Koziej, 1988; Pierre & Azzopardi, 1988) and are not considered in the current work.

A brief description of the target galaxies and justification for their selection is given in Section 2, followed in Section 3 by a description of the HST data and reduction techniques. Our results are discussed in Section 4 and summarized in Section 5.

2. The galaxies

2.1. M 81

M 81 is the gravitationally dominant member of its group, consisting of about 30 various types of galaxies (Börngen et al. 1982, 1984; Karachentseva et al., 1985). The galaxy is a suitable object for this study because of: its close distance, $D = 3.6$ Mpc (Freedman et al., 2001); and small inclination, which provide an opportunity to study the geometry of the stellar structures across the disk plane.

While young stellar populations of M 81, is situated mainly in spiral arms, have been extensively studied in numerous investigations, little is known about the galaxy periphery. Its optical surface brightness profile have been traced to $25 - 26^m/\square''$ limiting isophotes only (Tenjes et al., 1998), corresponding to angular major and minor axis diameters of about $24' \times 14'$. The surface brightness color index is unreliable indicator of different stellar populations. For example, the AGB and RGB stars, which differ in age, may have almost the same color, and therefore it become difficult to determine the age of the observed structures. Since spectral observations of outer regions are impossible due to the low surface brightness, the stellar photometry is the only method for the study the outer stellar structures.

The radio observations of M 81 revealed hydrogen bridges from M 81 to the neighboring galaxies M 82, NGC 2976, and NGC 3077 (van der Hulst, 1978; Appleton et al., 1981; Yun et al., 1994; Westpfahl et al., 1999; Boyce et al., 2001). The long gaseous filaments, generated in galaxies interaction, are gravity unstable and they might be fragmented to isolated systems, forming young Tidal Dwarf Galaxies (TDG) (Barnes & Hernquist, 1992; Elmegreen et al., 1993; Duc et al., 1998; Weilbacher, 2002). TDG candidates are discovered in many interacting pair of galaxies (Deeg et al., 1998; Hunsberger et al., 1996). It have been suggested that dwarf galaxies Ho IX, Garland, BK3N, observed within the hydrogen bridges of M 81, may be some of them (Miller, 1995; Flynn et al., 1999; Boyce et al., 2001). By comparing the results of observations with theoretical isochrones, Sakai & Madore (2001) concluded that the age of young stars in Garland is less than 150 Myr. The star formation history of Ho IX, Garland and BK3N, estimated from the single-star photometry of the HST images (Makarova et al., 2002), confirm the intensive star for-

mation in these galaxies on the time scale of 50-150 Myrs. In their study, however, the possible presence of the outer stars from the neighboring M 81 and NGC 3077 have not been considered. The underlying stellar population with ages more than 1 Gyr, observed by Makarova et al. (2002), is actually may be related to the outskirts of M 81 and/or NGC 3077 than to the underlying stellar population of the studied galaxies.

2.2. NGC 55

The spiral SB(s)m galaxy NGC 55 (Fig.2) is a member of the Sculptor group, consisting of approximately 30 galaxies (Cote et al., 1997; Jerjen et al., 2000). Since the galaxy is seen almost edge-on (Table 1), it is a convenient object for studying the spread of the thick disk and halo perpendicular to a disc plane. There are several distance estimations for NGC 55: e.g., Graham (1982) measurement of $D = 1.45$ Mpc, were based on the tip of the red giant branch method (TRGB); Pritchett et al. (1987) obtained $D = 1.34$ Mpc using photometry of Carbon stars. We estimated the distance to NGC 55 as 2.1 Mpc that differs considerably from those results.

The galaxy's neutral hydrogen disk has an angular size of about $45 \times 12'$ (Puche et al., 1991). It is plausible that part of this gas was driven out by the stellar winds during galaxy evolution. It would be valuable in future researcher to check the existence of galaxy stars on the galactocentric distances comparable to the extend of hydrogen disk. It has been also reported detection of a large diffused structure which extends up to about 3 kpc above the disk of NGC 55 seen in Chandra X-ray, VLT $H\alpha$, and Spitzer FIR emission. (Oshima et al., 2002; Otte & Dettman, 1999; Engelbracht et al., 2004)

2.3. NGC 300

The spiral galaxy SA(s)d (NED) NGC 300 is another member of the Sculptor group. Graham (1982) assumed that NGC 300 located on the same distance as NGC 55, i.e. $D = 1.45$ Mpc. Later, Graham (1984) estimated the distance $D = 1.65$ Mpc using photometry of Cepheids. The recent accepted distance is $D = 2.1$ Mpc, based also on the Cepheids photometry (Freedman et al., 1992). We have analyzed HST images of NGC 300 to measure distance to this galaxy, by on the TRGB method (Lee et al., 1993). The derived distance, $D = 2.00 \pm 0.13$ Mpc, is close to the value of Freedman et al. (1992). The brightest stars of NGC 300 have been studied spectroscopically for the identification of blue supergiants and determining a metallicity gradient along the galaxy disk (Bresolin et al., 2002). Using the value of the colors of RGB stars of the disk or the halo we are able to track the surface number density and metallicity gradients for the fainter and at least to Gyr elder.

The low inclination of NGC 300 (see Table 1) allows us to investigate both central part of the galaxy and its periphery. NGC 300 has a large hydrogen disk, $55' \times 50'$ (Rogstad et al., 1979; Puche et al., 1990) – it extended far more than visual part of the galaxy. The central part of NGC 300 is studied in detail, like for most of other galaxies, but the information about outer stellar population is scarce.

3. Observations, data reductions and analysis.

3.1. HST WFPC2 and ACS/WFC observations

To study the resolved stellar population of galaxies, we obtained all available HST archival images of 9 of M 81, 3 WFPC2 and 6 ACS/WFC regions of NGC 300 and 3 fields around of NGC 55. Digital Sky Survey images of these galaxies and WFPC2 & WFC footprints are shown in Fig. 1,2,3. The data of observation are listed in Table 2, where R is the angular separation in arcminutes between the observed field and the galactic center, ID is the program number and N_{stars} is the number of detected stars. Images were reprocessed through the standard WFPC2 and ACS STScI pipeline, as described by Holtzman et al. (1995a). After removing cosmic rays, we applied point-spread function (PSF) fitting packages DAOPHOT and ALLSTAR in MIDAS (Stetson, 1994). These programs use an automatic star-finding algorithm, followed by measurements of their magnitudes via PSF-fitting that is constructed from the isolated 'PSF-stars'. For the WFPC2 data we applied the aperture correction from the 1.5 pixel radius aperture to the standard $0''.5$ radius aperture size for the WFPC2 photometric system using the PSF-stars. The F555W, F606W and F814W instrumental magnitudes has been transformed to standard magnitudes in the Kron-Cousins system using the prescriptions of Holtzman et al. (1995b). The background galaxies, unresolved blends and stars contaminated by cosmetic CCD blemishes were eliminated from the final lists, using their “quality” ALLSTAR parameters, $|SHARP| > 0.3$, $|CHI| > 1.2$. We used ACS photometric instrumental magnitude scale, without transformation to Kron-Cousins system.

3.2. Method and star selection.

The primary goal of this study is to determine the basic morphological and chemical properties of the outer stellar surroundings of the target spiral galaxies. Using color-magnitude diagrams and stellar luminosity functions, we separated different stellar populations and analyzed their spatial distribution. We have compared stellar population characteristics of available fields differentially, avoiding some the complications of comparisons with stellar evolution models. Because the RGB loci for old stars are far more sensitive to metallicity than age, we use them to construct a first-order metallicity distribution functions, neglecting some known age-metallicity degeneracy. The spectroscopy of individual

thick disk/halo stars will be needed to break the age-metallicity degeneracy inherent to broad-band RGB colors.

Since the purpose of our research was to define stellar density at different distances from the center of a galaxy and to calculate the change of this density, we should be sure that various selection effects do not influence the received results or at least that their influence is insignificant. For this the following considerations were taken into account:

(i) We used images of different HST programs. It is natural therefore that exposition times and bands could have been various for different fields. To exclude an influence of exposition time on number of stars found in a field we were taking into account results received with the shortest exposition. We established the same threshold of luminosity of stars on all CM diagrams and excluded stars that had luminosity below this threshold, even if faint stars were visible in some images.

(ii) By removing the cosmic ray traces, we decreased their influence on the stellar counts. This step is important in sparse fields of halo, where the number of residual cosmic rays is comparable to the number of faint stars. To exclude the possible influence of cleaning for cosmic rays on the star counting, we selected stars which are a magnitude brighter than a photometric limit. As a result, the reduced number of stars increases the statistical fluctuations, but the number density of stars are less influenced by residual traces of cosmic rays.

(iii) The completeness of stars detection, especially at faint levels, is also effected by crowding of stars, which increases towards galaxy center. We performed the artificial star trials to correct the number density for the incompleteness.

(iv) Due to some inclination of the observed galaxies, it is important also to correct the measured stellar counts for the azimuthal position of the field. While changes in thickness of the disk might influence the results, it shouldn't significantly change the radial gradients.

(v) We excluded from our analysis the central galactic areas due to difficulties with the separation of evolved bulge stellar populations from the thick disk and halo ones.

Another concern here is our ability to distinguish by multi-color photometry alone a grouping of stars in the thick disk/halo from the plethora of stars found in the galaxy's enveloping thin disk. Can we separate the AGB and RGB stars between these two disks? For the high-inclination systems, as NGC 55, this selection is evident, since at large distances from disk plane the thick disk is a dominant contributor of stars. Several studies have shown that thick disk/halo stars are uniformly elder and more metal poor than thin disk ones (Gilmore & Wyse 1985; Carney et al. 1989). If the thick disk stars are uniformly old, then any star whose life expectancy is brief will necessary belong to the thin disk, regardless of its kinematics or metallicity. By sorting stars on the different

groups according to their life expectancies, we can assign probable membership of stars to the thin disk or thick-disk populations. The measurements of the stellar density along galaxy radius on the border of the thin disk may clarify this question. In one of our cases (see section 4.3), the density of RGB stars decreases monotonously and does not uncover the border of the thin disk.

We have not considered the AGB stars as a good tracer of a thick disk. The relative density of the AGB stars in comparison with RGB stars are lower and their evolutionary status is less certain. Although, sometimes they are a good indicator of the edge of the thin disk.

4. Results

4.1. CM Diagrams of M 81, NGC 55 and NGC 300.

The results of stellar photometry are presented on the CMDs (Fig. 4 and 5). The features of these diagrams resemble those of other spiral galaxies, however, there are some systematic differences between CMDs of various fields. It can be explained by the distinction of distances between the fields and the galaxy center. Indeed, some fields are situated in spiral arms, but others are outside of a visible disk. As a result, the relationship between number of old and young stars on CM-diagrams of different fields varies from one to the other. The dashed line in all the presented CMDs indicates the position of the tip of the red giant branch (TRGB).

4.2. Distances

The errors in distances of investigated galaxies do not significantly affect our major aim, constraining the relative stellar density distribution. In the context of distance verification, it is important to compare different methods. At the same time, it allows us to estimate distance moduli to the galaxies using the dereddened magnitude of the tip red giant branch (TRGB) (Lee et al., 1993). This method has distance uncertainties less than 10% which is comparable with the best Cepheid distances. To the author's knowledge, this is a first measurement of M 81 and NGC 55 distances based on this method. As it was shown in several studies the distance estimated with the Cepheids method can significantly differ from the TRGB and other methods. For example, in case of well studied M 33 the disagreement between two methods is $\sim 0^m3$ in distance modulus, which is a large value for the galaxy located in the Local Group (Lee et al. 2002; Kim et al. 2002). Therefore, it is necessary to compare different distance indicators in other galaxies to reveal possible reasons of such dispersion.

In order to estimate distances, we have used one or several fields for each galaxy, avoiding star formation regions with bright supergiants. We preferred fields with large

number of red giant to decrease statistical error of TRGB method. These fields are - S2, S3, S4, S5, S6 for M 81 (Fig.1), S3 for NGC 55 (Fig.2) and S1 for NGC 300 (Fig.3). CM diagrams of these fields are shown in Figs. 4 and 5. A typical samples of incompleteness of such fields are shown in Figs. 6 and 7. The stellar luminosity function of such field has a gap which corresponds to the tip of red giant branch (TRGB)(see Fig.8). Using the method of Lee et al. (1993), we have estimated distances to galaxies and mean metallicity of red giants. The extinction coefficients of all galaxies were taken from the study of Schlegel et al. (1998).

Our values for M 81 are following: field S2 $(m - M) = 27.89 \pm 0.10$, field S3 - $(m - M) = 27.89 \pm 0.10$, field S4 - $(m - M) = 27.95 \pm 0.10$, field S5 - $(m - M) = 27.95 \pm 0.10$ and field S6 - $(m - M) = 27.95 \pm 0.10$. The metallicity of inner fields (S2, S3, S5, S6) varies from -0.6 to -0.7 , while the metallicity of outer field S4 is $[Fe/H] = -0.77$. We estimated mean distance modulus for M 81 as $(m - M) = 27.93 \pm 0.04$ (that corresponds to $D = 3.85 \pm 0.08$ Mpc) which is very close to the mean distance of 16 dwarf galaxies of the group, $(m - M) = 27^m9$, determined with TRGB method (Caldwell et al. 1998, Karachentsev et al. 2002). This indicates that M 81 is near the center of the group and there is no asymmetry of spatial distribution of galaxies in the group.

The previous distance estimation to the galaxy M 81 was determined from the Cepheids photometry (Freedman et al., 1994): $(m - M) = 27.80 \pm 0.20$. This value was corrected in later studies of Freedman et al. (2001) to $(m - M) = 27.75 \pm 0.08$. Significant disagreement between TRGB and Cepheid distances, 0^m18 , are above the estimated errors and not correlated with metal content.

For NGC 55 (field S3) we estimated following values: $(m - M) = 26.64 \pm 0.10$, $D = 2.12 \pm 0.10$ Mpc and $[Fe/H] = -1.25$. Our distance estimation differs essentially from the value of Puche et al. (1991) $D = 1.6$ Mpc but it is in accordance with the suggestion of Graham (1982) that galaxies NGC 55 and NGC 300 are at the same distance.

For NGC 300 (field S1) we estimated following values: $(m - M) = 26.50 \pm 0.15$, $D = 2.00 \pm 0.13$ Mpc, and $[Fe/H] = -0.87$. The distance is very similar to the one estimated by Freedman et al. (2001) $(m - M) = 26.53 \pm 0.07$ ($D = 2.02$ Mpc), which was estimated by Cepheids photometry method.

4.3. Metallicity gradient of the RGB stars along galactocentric radius.

The metallicity gradients along the galactocentric radius are observed as in our Galaxy and other spiral galaxies, Currently, the MDs are obtained from spectroscopic observations of stellar clusters (Friel & Janes, 1993; Rolleston et al., 2000) and HII regions (Shaver et al., 1983; Marquez et al., 2002). Only nearby galaxies are accessible for spectral metallicity measurements of old stellar population (red-giants) due to low luminosity of

studied stars (Reitzel & Guhathakurta, 2002). In resolved galaxies an average metallicity of red giants is estimated using a position of the red giants branch on a CM diagram (Lee et al., 1993). The advantage of this method is that red giants can be seen on relatively large distances from galactic center, where a surface brightness is very low and spectral methods are inapplicable.

Perhaps the most noticeable metallicity-age gradient is observed in M 81, based on the comparison of the mean colors of the RGB locus from different fields. The mean metallicity of red giants in the S2, S3, S5, S6 fields is $[Fe/H] = -0.65 \pm 0.03$. For the field S4, which has a larger galactocentric distance (Fig. 1) the mean RGB metallicity is $[Fe/H] = -0.77$.

The metallicity gradient of the galaxy NGC 300 in the fields S1 and F4 is well seen in Fig. 9, where maximum of star distribution corresponds to the position of red giants branch. This maximum is changed from $(V - I) = 1.40$ to $(V - I) = 1.48$ along galactocentric radius, that corresponds to increasing of metallicity. We investigated the color of RGB stars throughout the thin disk of NGC 300 using the ACS/WFC and WFPC2 images and found that there is a presence of a color gradient of RGB stars at the edge of thin disk (fields S1 and F4) and near the center of the galaxy (Fig.9). The decreasing of the color index to the center of galaxy may be a summary effect of the age and metallicity of red giants. Thus the number of the red giants with a lower metallicity or with less average age increases near the center of galaxy. At the edge of the galaxy the colour index decrease can be explained only by the decrease of the metallicity along radius, because the age of red giants can not decrease at the periphery without signs of star formation processes. The color index and then the metallicity of the red giants along thin disk body has no considerable changes.

The measurements of the edge-on galaxy NGC 55, demonstrated a very low metallicity gradient. This probably due to the fact, that measurements have been performed along the small axis of the galaxy, but not along the radius.

4.4. *Surface density of AGB and RGB stars in galaxies.*

The main goal of the this paper is to study of stellar distribution around spiral galaxies. Earlier, on basis of the study of 16 irregular dwarf galaxies, we discovered that red giants form a thick disk around each galaxy. The size of such disk is 2-3 times larger than those of visible part of the galaxy (Tikhonov, 2002). We did not detect stars that belong to the galaxy beyond of these disks. At the same time, our study of a more luminous irregular galaxy IC10 demonstrated that it has an extended disk (Tikhonov, 1999) and a more extended halo behind the sharp edge of this disk (Tikhonov, 2002; Drozdovsky et al., 2002). It is interesting, that the red giants of IC 10's disk and halo demonstrate different

gradients of stellar density. A sharp border between thick disk and the halo is detected in galaxy M 33 (Guillandre et al., 1998). However, the authors did not measure the density gradients of red giants in the thick disk and the halo. The surface distribution of various objects in M 31 was investigated by Ferguson et al. (2002) on the basis of wide field images. It was discovered that the stellar density as well as the mean metallicity vary along the galaxy radius.

The main problem encountered during data processing was casual location of observed fields that were analyzed in spatial star distribution study. We assumed that disk and halo have an axially symmetric shape without any tidal deformation. Since galaxies have an inclination to the line of sight, we calculated the distance from the investigated area to the galactic center with the following equation:

$$Radius = \sqrt{(D_a)^2 + (D_b/\cos A)^2}, \quad (1)$$

where D_a is a projection of the seen distance from the investigated area to the galaxy center on the large galaxy axis, D_b is the same projection on the small axis of the galaxy, and A is the galaxy inclination angle to the line of site. In this way, distances for all fields of M 81 were calculated and the distribution of stars along the galaxy radius was constructed. However, before constructing the distribution, we performed a selection of objects and stars number correction for the incompleteness of sample as described in section 2.2.c.

4.5. M 81.

The studied fields are situated in the galaxy periphery as well as in the spiral arms (see Fig. 1), where star density is high. A few bright supergiants makes photometry of faint objects (such as red giants) more complicated and decreases the sample completeness. On the basis of artificial star trials we calculated the incompleteness curves for all studied fields, and corrected the measured stellar number density for this effect. In Fig. 6, we present results for two typical fields, S3 and S4. For M 81 we used red giants in magnitude range as follows: $24^m0 < I < 25^m0$ and $25^m5 < V < 26^m5$. From the mentioned above plots (Fig.6), we found that in case of field S3 sample completeness is 0.80 for I band and 0.35 for V band. In case of field S4, the completeness is 0.95 and 0.90, respectively, and corrections for incompleteness are minor. The AGB stars are more luminous than RGB ones and incompleteness correction is very small. To increase statistical significance of results, we estimated a mean number density of stars (AGB and RGB) for each of the three chips of WFPC2 (except small PC chip). The achieved results are presented in Figures 10 and 11. These figures demonstrate a visible bend of star density distribution. This bend correspond to a border between the thick disk and the halo. It's clearly seen that RGB stars demonstrate lower density gradient than that of the AGB stars. These

gradients difference causes variation of RGB/AGB stars ratio along the galaxy radius. The radius of thick disk of M 81 galaxy is equal to $22'$ (see Fig.11) which corresponds to 25 kpc. The images that have been analyzed do not allow to reach the outer part of the halo. Its radius is not less than 40 kpc. A similar extended halo is observed in M 31 (Ferguson et al., 2002) and NGC5128 (Harris et al., 1999). On some of our images there are not only stars of M 81's disk and halo, but also stars of dwarf galaxies BK3N, Ho IX, Arp's ring can be seen. Such objects are well seen in Figure 10, where demonstrates distribution of stars along the galaxy radius. These objects lie above the general dependence line.

From figures 10 and 11, one can conclude that in dwarf galaxies BK3N and Ho IX present AGB stars but are absent the elder RGB stars, which is in accordance with assumption that these galaxies are young tidal formations (Miller, 1995; Flynn et al., 1999; Boyce et al., 2001). The lack of RGB stars creates a difficulty to estimate distances. The distance values obtained by Karachentsev et al. (2002) refer to halo and disk stars of M 81, but not to BK3N and Ho IX. In Arp's ring field both AGB and RGB stars are presented (Fig.10, 11). Since RGB stars are at least 1-2 Gyr old, the age of Arp's ring can not be younger. Its CM diagram has blue stars that indicate that there are some low star formation in the ring.

4.6. NGC 300.

Three WFPC2 fields that we have analyzed for studying of the stellar density, are situated nearly along the galaxy diameter (Fig. 3). Therefore the galaxy inclination correction is the same for all the fields. We did not correct the galaxy inclination as in the case of M 81. It is well seen (Fig. 12), that the thick disk and the halo demonstrate different gradient of star density decrease. As in the case of M81, the stellar density of the thick disk, can be presented by exponential form (Fig. 12). The thick disk of NGC 300 has a well seen border, although as well as in the case of M 81 halo border can not be determined. As shown in Fig. 12, the halo sizes measured by us almost two times larger than that of main galaxy body. On the true-color picture of NGC 300 (MPG/ESO 2.2-m + WFI) a bluish disk with the sharp border on its outskirts can be seen. All spiral arms are embedded into this disk. Usually size of such disks are considered as a visual size of the galaxy. Field S2 is situated on the edge of this bluish disk where all variations of stellar population can be studied. The number of blue stars (main sequence giants and supergiants) rapidly decreases on the edge of thin disk up to zero (see Fig.13). The number of AGB stars also decreases nearly to zero, but red giants of thick disk do not demonstrate the evident variation of star density on the edge of thin disk and extended over blue disk borders. However, the diameter thick disk is only 1.2 times larger than that of the thin disk of the galaxy (Fig. 13).

4.7. NGC 55.

NGC 55 is edge-on galaxy and we can investigate its stellar density along Z-axis, i.e. perpendicular to the plane of the disk. On the basis of three regions which are situated on different distances from the plane of the galaxy, we determined the density of the red giants along Z axis from 2 to 7 kpc. It was found that all the regions (S1, S2, S3) demonstrate the same behavior of the decreasing of the red giants density, i.e. all fields are in the thick disk. Surprising is the fact, that fields S2 and S3 are situated at different radii of the galaxy (Fig. 2), but both demonstrate the same dependence of the decreasing of the red giants density along small axis. A shape of Density-Radius relation (Fig. 14) is not the same as for M 81 and NGC 300 galaxies: we did not see the transition from the thick disk to the halo. This effect can be explained by the fact that none of the three fields reached the disk edges, half thickness of that is no less than 6 kpc. Perhaps, the deviation of density distribution from the straight line (Fig. 14) correspond to the transition from the disk to the halo, but on the other hand, it can be only a fluctuation of density in the disk. To determine the precise disk size and to reveal the halo, additional observations should be performed. We have no images of NGC 55 along large axis, so that to trace change of the density of the red giants in this direction. However, assuming that the decrease of the density of red giants in this direction is going the same manner as along small axis, we can estimated that the ratio of axes of the thick disk roughly is equal to 2.5 : 1, which is a mean value for irregular galaxies (Tikhonov, 2002).

As in M 81, the AGB stars in NGC 55 and NGC 300 has a stronger surface density gradient, than the density gradient of RGB stars. As a result on CMDs from periphery of galaxies we mostly see RGB stars and only few AGB and other field stars. Due to the small statistics of the AGB stars in our data of NGC 55 and NGC 300, the significance of their gradient density calculations is low.

5. Discussion.

On the basis of the study of star density in the three spiral galaxies, we examine the spatial distribution of stars in a region of their thick disks and halos. The disks and halos of M 81 and NGC 300 have similar structure, but differ in spatial sizes. In the NGC 55 we see a thick disk and we can only assume the presence of the halo. On the basis of our results, an appropriate model of the stellar structure of the spiral galaxy is presented (Fig. 15). We have no means to probe at this study the young stellar populations and gaseous component of the galaxies. The thin disk thickness depends of galaxy's type (Ma, 2002). Approximate thickness of the thin disk in M81, NGC 55 and NGC 300 is 1.5-0.7 kpc. The thick disk, as seen at NGC 55 (Fig.14), has thickness 13 kpc, but the ratio of thick-to-thin diameters is only 1.2 – 1.3. The same ratio is observed at M 33 (Guillandre

et al., 1998). By comparing a stellar structure of galaxies M 81 and NGC 300 with ones of irregular galaxies (Tikhonov, 2002) we can see a certain dependence: while spiral galaxies have a ratio of sizes of thick disks to visible disks to 1.2 – 1.3, irregular galaxies demonstrate this ratio from 2.5 to 5. A very large red giants disk was found in the dwarf lenticular galaxy NGC 404 (Tikhonov et al., 2003). It is possible that all spiral galaxies have not only a thick disk but also an extensive halo, while dwarf irregular galaxies have only a thick disk. Knowing that bright irregular galaxy IC 10 has a thick disk and an extended halo (Drozdovsky et al., 2003), we can assume that there is a dependence between the mass of the galaxy and availability of its halo. Elliptical shape of halo in fig.15 is a result of our investigation of spiral edge-on galaxies NGC 891, NGC 4144 and IC 5052 which will be published later. This elliptical shape have also the halo of spiral galaxy M 31 (Zucker et al., 2004). In order to come to statistically reliable conclusions, it is necessary to study stellar periphery of some nearby galaxies with different masses.

At the moment, there are several theories of formation of stellar halo in galaxies (Bullock et al., 2001 and references therein). Our results can not be used as perfect basis for some kind of theory of halo formation due to small number of studied galaxies and we do not compare our results with theories. To all appearance, we can not consider halo as a far extension of the bulge, because in the NGC 300 we see a very little bulge, but the halo is large enough.

6. Summary.

By resolving galaxies onto single stars and studying spatial distribution of various types of stars, it allows us to mark out spatial structures in galaxies and determine its properties. The method of stellar density allows to reveal galactic structures of very low surface brightness, which is not possible with the method of surface photometry. On the basis of stellar density method we have obtained following new results:

a) The stellar thick disks and halo are revealed in galaxies M 81, NGC 300 and NGC 55.

b) It is pointed out that decreasing of stellar density in the thick disks and halo of spiral galaxies occurs by different gradients, that let us to determine the border between halos and thick disks.

c) The distances to M 81, NGC 55 and NGC 300¹ are estimated on the basis of red giants photometry.

¹ Under submitting the paper to A&A we found the very new paper (astro-ph/0312007) about of stellar content of NGC 300. Authors used the same HST archive data as ours and estimated the distance to NGC 300 with a good accordance of ours result.

d) The existence of metallicity gradient of old stars in thick disks of spiral galaxies is confirmed.

At present, the extensive archive of HST images allows to investigate spatial distribution of stellar population at least in several galaxies. The results of this study can be applied for the modeling galactic structure. Moreover, the presence of extended thick disk and halo in galaxies is valuable for the study of dark matter. We hope that our results will be helpful in solving these problems.

Acknowledgements. The authors would like to thank to the Russian Foundation for Basic Research for financial support under the grant 03-02-16344. Data from the NASA/IPAC Extragalactic Database have been used.

References

- Appleton P.N., Davies R.D., Stephenson R.J., 1981, MNRAS 195, 327
- Baggett W.E., Baggett S.M., Anderson K.S.J., 1998, AJ 116, 1626
- Barnes J.E. & Hernquist L., 1992, Nature 360, 715
- Bellazzini M., Cacciari C., Federici L., Fuci Pecci F., Rich M., 2003, A&A 405, 867
- Boyce P. J., Minchin R. F., Kilborn V. A., Disney M. J., Lang R. H., Jordan C. A., Grossi M., Lyne A. G., Cohen R. J., Morison I. M., Phillipps S., 2001, ApJ 560L, 127
- Börngen F., Karachentseva V. E., Schmidt R., Richter G. M., Thaenert W., 1982, AN 303, 287
- Börngen F., Karachentseva V. E., Karachentsev I. D., 1984, AN 305, 53
- Bresolin F., Gieren W., Kudritzki R.-P., Pietrzyński G., Przybilla N., 2002, ApJ 567, 277
- Brewer M.-M., Carney B.W., 2004, PASA, 21, 134
- Brewer J., Richer H., Crabtree D., 1995, AJ 109, 2480
- Brown T.M., Ferguson H.C., Smith Ed., Kimble R.A., Sweigart A.V., Renzini A., Rich R.M., VandenBerg D. A., 2003, ApJ 592, L1
- Bullock J.S., Kravtsov A.V., Weiberg D.H., 2001, ApJ 548 ,33
- Burkert A., Truran J. W., Hensler G., 1992, ApJ 391, 651
- Byun Y.I. & Freeman K.C., 1995, ApJ 448, 563
- Caldwell N., Armandroff T.E., Da Costa G.S., Seitzer P., 1998, AJ 115, 535
- Carney B.W., Latham D.W., & Laird J.B., 1989, AJ 97, 423
- Chiba M. & Beers T.C., 2000, AJ 119, 2843
- Cote S., Freeman K., Carignan C., Quinn P., 1997, AJ 114, 1313
- Dalcanton J.J. & Bernstein R.A., 2002, AJ 124, 1328
- Deeg H.J., Munoz-Tunon C., Tenorio-Tagle G., Telles E., Vilchez J. M., Rodriguez-Espinosa J. M., Duc P. A., Mirabel I. F., 1998, A&AS 129, 455
- Drozdovsky I., Tikhonov N., Schulte-Ladbeck R., "The outer stellar edges of irregular galaxies: IC10 and LeoA", 2003, STSci May 2003 Symposium
- Drozdovsky I., Schulte-Ladbeck R., Tikhonov N., "The outer edges of dwarf irregular galaxies: stars and gas", 10-11 October, 2002, Lowell Workshop
- Duc P.-A., Mirabel I.F., 1998, A&A 333, 813

- Eggen O.J., Lynden-Bell D. & Sandage A.R., 1962, *ApJ* 136, 748
- Elmegreen B.G., Kaufman M., Thomasson M., 1993, *ApJ* 412, 90
- Engelbracht C. W., MIPS Science Team, SINGS Team, 2004, *AAS* 204, 3311
- Ferguson A. M. N. & Johnson R.A., 2001, *ApJ* 559L, 13
- Ferguson A. M. N., Irein M. J., Ibata R.A., Lewis G.F., Tanvir N. R., 2002, *AJ* 124, 1452
- Friel E.D. & Janes A., 1993, *A&A* 267, 75
- Flynn L., Walterlos R.A.M., Thilker D.A., Fierro V., 1999, 5-9 January, *AAS Meeting* 193 - Austin, Texas
- Freedman W.L., Madore B.F., Hawley, S. L.; Horowitz I. K., Mould J., Navarrete M., Sallmen S., 1992, *ApJ* 396, 80
- Freedman W.L., Hughes S.M., Madore B.F., 1994, *ApJ* 427, 628
- Freedman W.L., Madore B. F., Gibson B. K., Ferrarese L., Kelson D. D., Sakai S., Mould J. R., Kennicutt R. C. Jr., Ford H. C., Graham J. A., Huchra J. P., Hughes S. M. G., Illingworth G. D., Macri L. M., Stetson P. B., 2001, *ApJ* 553, 47
- Georgiev Ts. B., Bilkina B.I., Tikhonov N.A., 1992, *A&AS* 95, 581
- Georgiev Ts. B., Bilkina B.I., Tikhonov N.A., 1992, *A&AS* 96, 569
- Gilmore G., & Wyse R.F.G., 1985, *AJ* 90, 2015
- Gilmore G., Wyse R.F.G., & Norris J., 2002, *ApJ* 574, L39
- Graham J.A., 1982, *ApJ* 252, 474
- Graham J.A., 1984, *AJ* 89, 1332
- Guillandre J., Lequeux J., Loinard L., 1998 in *IAU Symp. 192, The Stellar content of Local Group Galaxies*, ed. Whitelock P., Cannon R., 27
- Harris W.E. & Harris G. L. H., 2001, *AJ* 122, 3065
- Harris G., Harris W., Poole G., 1999, *AJ* 117, 855
- Holtzmann J.A., Hester J.J., Casertano S., 1995a, *PASP* 107, 156
- Holtzmann J.A., Burrows C.J., Casertano S., Hester J.J., Trauger J.T., Watson A.M., & Worthey G., 1995b, *PASP* 107, 1065
- Hunsberger S.D., Chareton J.C., Zaritsky D., 1996, *ApJ* 462, 50
- Harris W. E., Harris G.L.H., 2001, *AJ* 122, 3065
- Jerjen H., Binggeli B., Freeman K., 2000, *AJ* 119, 593
- Ibata R.A., Gilmore G., Irwin M.J., 1995, *MNRAS* 277, 781
- Karachentsev I. D., Dolphin A. E., Geisler D., Grebel E. K., Guhathakurta P., Hodge P. W., Karachentseva V. E., Sarajedini A., Seitzer P., Sharina M. E., 2002, *A&A* 383, 125
- Karachentseva V. E., Karachentsev I. D., Boerngen F., 1985, *A&AS* 60, 213
- Kent S.M., 1985, *ApJS* 59, 115
- Kim M., Kim E., Lee M. G., Sarajedini A., Geisler D., 2002, *AJ* 123, 244
- Kiszkurno-Koziej E., 1988, *A&A* 196, 26
- Lee M.G., Freedman W.L., Madore B.F., 1993, *AJ* 417, 553
- Lee M.G., Kim M., Sarajedini A., Geisler D., Gieren W., 2002, *ApJ* 565, 959
- Ma J., 2002, *A&A* 388, 389 Geisler D., 2000, *AJ* 119, 760

- Makarova L. N., Grebel E. K., Karachentsev I. D., Dolphin A. E., Karachentseva V. E., Sharina M. E., Geisler D., Guhathakurta P., Hodge P. W., Sarajedini A., Seitzer P., 2002, *A&A* 396, 473
- Marquez I., Masegosa J., Moles M., Varela J., Bettoni D., Galletta G., 2002, *A&A*, 393, 389
- Miller B.W., 1995, *BAAS* 185, 1365
- Oshima T., Mitsuda K., Ota N., Yamasaki N., 2002, The 8th IAU Asian-Pacific Regional Meeting, July 2-5, 2002, Tokyo, Japan, 287
- Otte B. & Dettmar R.-J., 1999, *A&A* 343, 705O
- Pierre M. & Azzopardi M., 1988, *A&A* 189, 27
- Prieto M., Aguerri J. A. L., Varela A. M., Munoz-Tunon C., 2001, *A&A* 367, 405
- Pritchett C. J., Schade D., Richer H. B., Crabtree D., Yee H. K. C. 1987, *ApJ* 323, 79
- Pritchett C.J. and van den Bergh S., 1988, *ApJ* 331, 135
- Prochaska J.X., Naumov S. O., Carney B. W., McWilliam A., Wolfe A. M., 2000, *AJ* 120, 2513
- Puche D., Carignan C., Bosma A., 1990, *AJ* 100, 1468
- Puche D., Carignan C., Wainscoat R. J., 1991, *AJ* 101, 447
- Reitzel D.B. & Guhathakurta P., 2002, *AJ* 124, 234
- Rogstad D.H., Crutcher R.M. and Chu K., 1979, *ApJ* 229,509
- Rolleston W.R.J., Smart S.J., Dufton P.L., Ryans R.S.I., 2000, *A&A* 363, 537
- Sakai S. & Madore B., 2001, *ApJ* 555, 280
- Sarajedini A., Geisler D., Schommer R., Harding P., 2000, *AJ* 120, 2437
- Sarajedini A. & Van Duyne J., 2001, *AJ* 122, 2444
- Searle L., Zinn R., 1978, *ApJ* 225,357
- Shaver P.A., McGee R.X., Danks A.C., Pottasch S.R., 1983, *MNRAS* 204, 53
- Schlegel D. J., Finkbeiner D.P.; Davis M., 1998, *ApJ* 500, 525
- Stetson, P.B. 1994, Users Manual for DAOPHOT II
- Tenjes P., Haud U., Einasto J., 1998, *A&A* 335, 449
- Tikhonov N.A., 1999, *IAUS*, 192, 244
- Tikhonov N.A., 2002, Dissertation, St-Petersburg State University, Russia
- Tikhonov N.A., Galazutdinova O.A., Aparicio A., 2003, *A&A* 401, 863
- Vallenari A., Bertelli G., Schmidtbreick L., 2000, *A&A* 361, 73
- Venn K.A., Irwin M., Shetrone M.D., Tout C.A., Hill V., Tolstoy E., astro-ph/0406120
- van der Hulst J.N., 1978, in *Structure and Properties of Nearby Galaxies*, IAU Symp., No.77, (Reidel, Dordrecht and Boston), 269
- van der Marel R.P. 2001, astro-ph/0107248
- Weilbacher P.M., 2002, PhD Dissertation, Notingen
- Westpfahl D. J., Coleman P. H., Alexander J., Tongue T., 1999, *AJ* 117, 868
- Williams B.F., 2002, *MNRAS* 331, 293
- Yun M.S., Ho P.T.P., Lo K.Y., 1994, *Nature* 372, 530
- Zickgraf F.-J., Humphreys R. M., Sitko M. L., Manley T., 1990, *PASP* 102, 925
- Zoccali M., Renzini A., Ortolani S., Greggio L., Saviane I., Cassisi S., Rejkuba M., Barbuy B., Rich R.M., Bica E., 2002, astro-ph/0210660

Zucker D.B., Kniazev A.Y., Bell E.F., Martinez-Delgado D., Grebel E.K., Rix H.-W., Rockosi C.M., Holtzman J.A., Waltherbos R.A.M., Ivezić Z., Brinkmann J., Brewington H., Harvanek M., Kleinman S.J., Krzesinski J., Long D., Newman P.R., Nitta A., Snedden S.A., 2004, astro-ph/0401098

Table 1. Properties of NGC 55, NGC 300, M 81 (from NED).

Galaxy	NGC 55	NGC 300	M 81
RA (J2000)	$00^h 14^m 54^s$	$00^h 54^m 54^s$	$09^h 55^m 33^s$
DEC (J2000)	$-39^\circ 11' 49''$	$-37^\circ 41' 00''$	$69^\circ 03' 55''$
Morphological type	SB(s)m:sp	SA(s)d	SA(s)ab:LINER Sy1.8
Helio radial velocity (km/s)	129 ± 3	144 ± 1	-34 ± 4
Diameter (arcmin)	32.4×5.6	21.9×15.5	26.9×14.1
Magnitude	$8^m 84$	$8^m 95$	$7^m 89$
A_V	$0^m 044$	$0^m 042$	$0^m 266$
A_I	$0^m 026$	$0^m 025$	$0^m 155$
Inclination	85°	40°	59°

The Galactic extinction correction by Schlegel et al.(1998).

The inclination taken from LEDA.

Table 2. Observational log of HST.

Galaxy	Region	Date	Band	R	Exposure	ID	N_{stars}	
M 81	S1	17.04.1998	F814w	2.96	1000+1200	7909	18164	
			F606w	2.96	2×1000	7909		
	S2	26.01.1999	F814w	5.18	3×1500	8059	22933	
			F606w	5.18	5×1500	8059		
	S3	4.06.2001	F814w	3.47	4×500	9073	19143	
			F555w	3.47	4×500	9073		
	S4	30.06.2001	F814w	12.78	3×1400	9086	1611	
			F606w	12.78	4×1300	9086		
	S5	1.09.2001	F814w	6.09	2×1100	8584	10150	
			F555w	6.09	2×1100	8584		
	S6	28.05.2002	F814w	9.52	800	9634	7810	
			F606w	9.52	2×500	9634		
	BK3N	29.08.2000	F814w	10.87	600	8061	519	
			F606w	10.87	600	8061		
Ho IX	27.06.2001	F814w	11.39	600	8061	3655		
		F606w	11.39	600	8061			
Arp's loop	30.07.2000	F814w	17.61	600	8061	956		
		F606w	17.61	600	8061			
NGC 300	S1	13.09.2001	F814w	7.12	2×500	8584	4387	
			F555w	7.12	2×500	8584		
	S2	02.07.2001	F814w	5.99	2×300	9162	12004	
			F606w	5.99	2×300	9162		
	S3	20.06.2001	F814w	12.83	4×500	9086	2520	
			F606w	12.83	4×500	9086		
	F1	17.07.2002	F555w	8.05	1080	9492	89615	
			F814w	8.05	1080	9492		
	F2	19.07.2002	F555w	2.07	1080	9492	182106	
			F814w	2.07	1080	9492		
	F3	28.09.2002	F555w	0.91	1080	9492	191107	
			F814w	0.91	1080	9492		
	F4	21.07.2002	F555w	8.97	1080	9492	53494	
			F814w	8.97	1080	9492		
	F5	25.12.2002	F555w	5.45	1080	9492	128370	
			F814w	5.45	1080	9492		
	F6	26.09.2002	F555w	6.15	1080	9492	68730	
			F814w	6.15	1080	9492		
	NGC 55	S1	13.06.2001	F814w	8.00	4×500	9086	832
				F606w	8.00	4×500	9086	

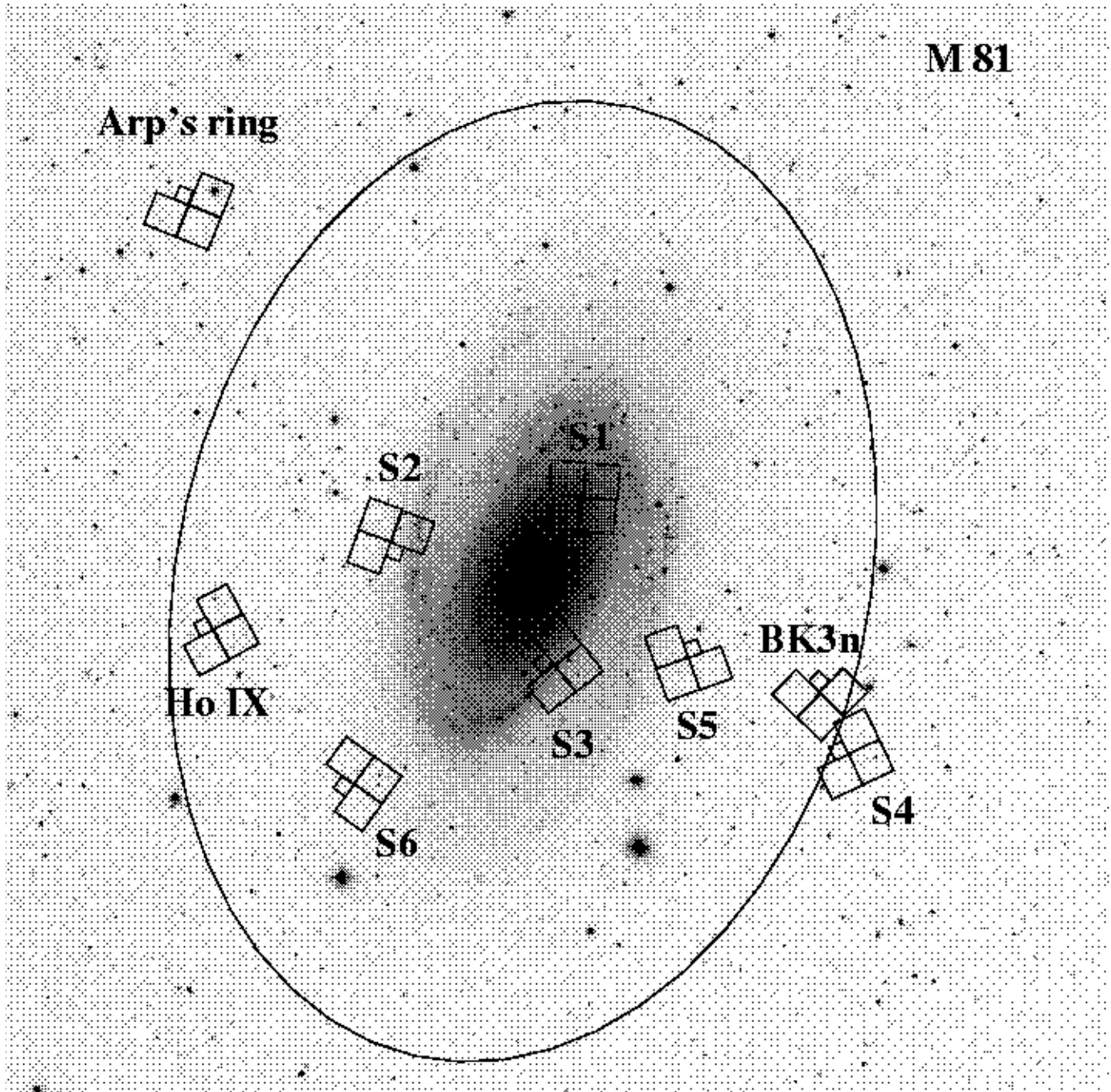


Fig. 1. DSS-2 $40' \times 40'$ image of M 81 the HST/WFPC2 footprints superposed, indicating 9 regions (S1, S2, S3, S4, S5, S6, BK3N, Ho IX, Arp' ring) observed. The edge of thick disk of red giants is marked by ellipse.

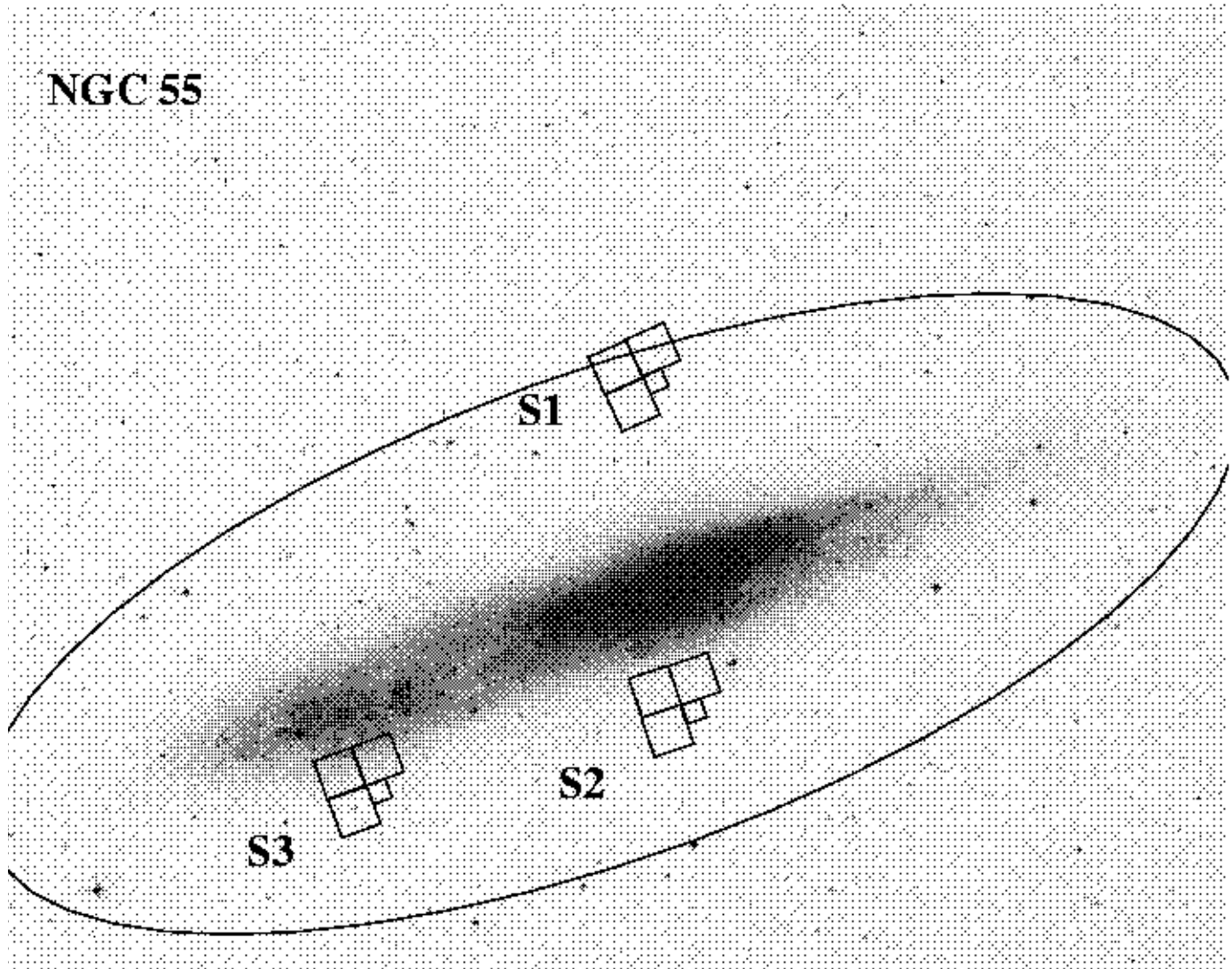


Fig. 2. DSS-2 $40' \times 40'$ image of NGC 55 the HST/WFPC2 footprints superposed, indicating the 3 regions (S1, S2, S3) observed. The edge of thick disk of red giants is marked by ellipse.

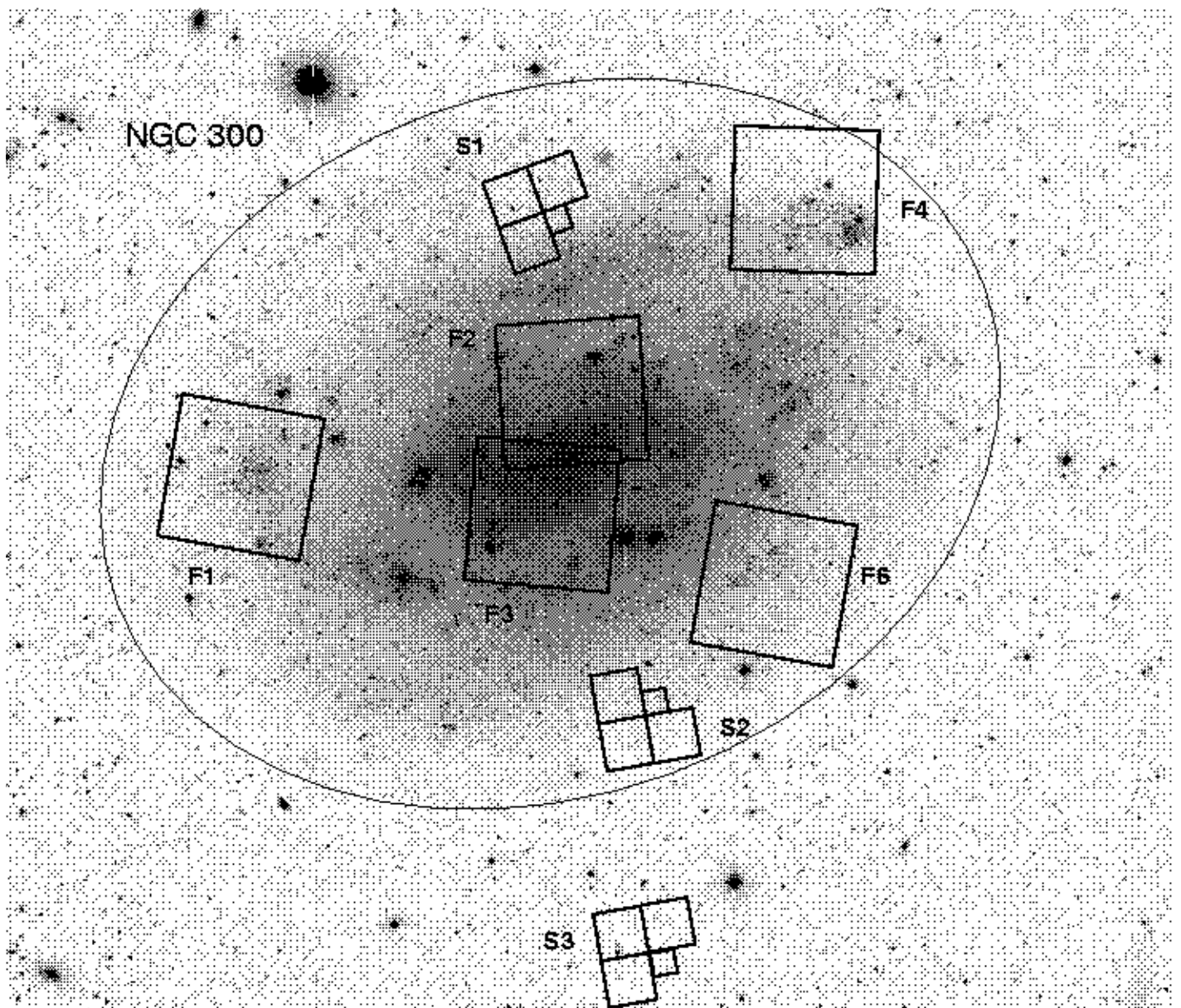


Fig. 3. MPG/ESO 2.2m telescope + WFI $34' \times 33'$ image of NGC 300 the HST/WFPC2 footprints superposed, indicating 9 regions (S1, S2, S3, F1, F2, F3, F4, F5, F6) observed. The edge of thick disk of red giants is marked by ellipse.

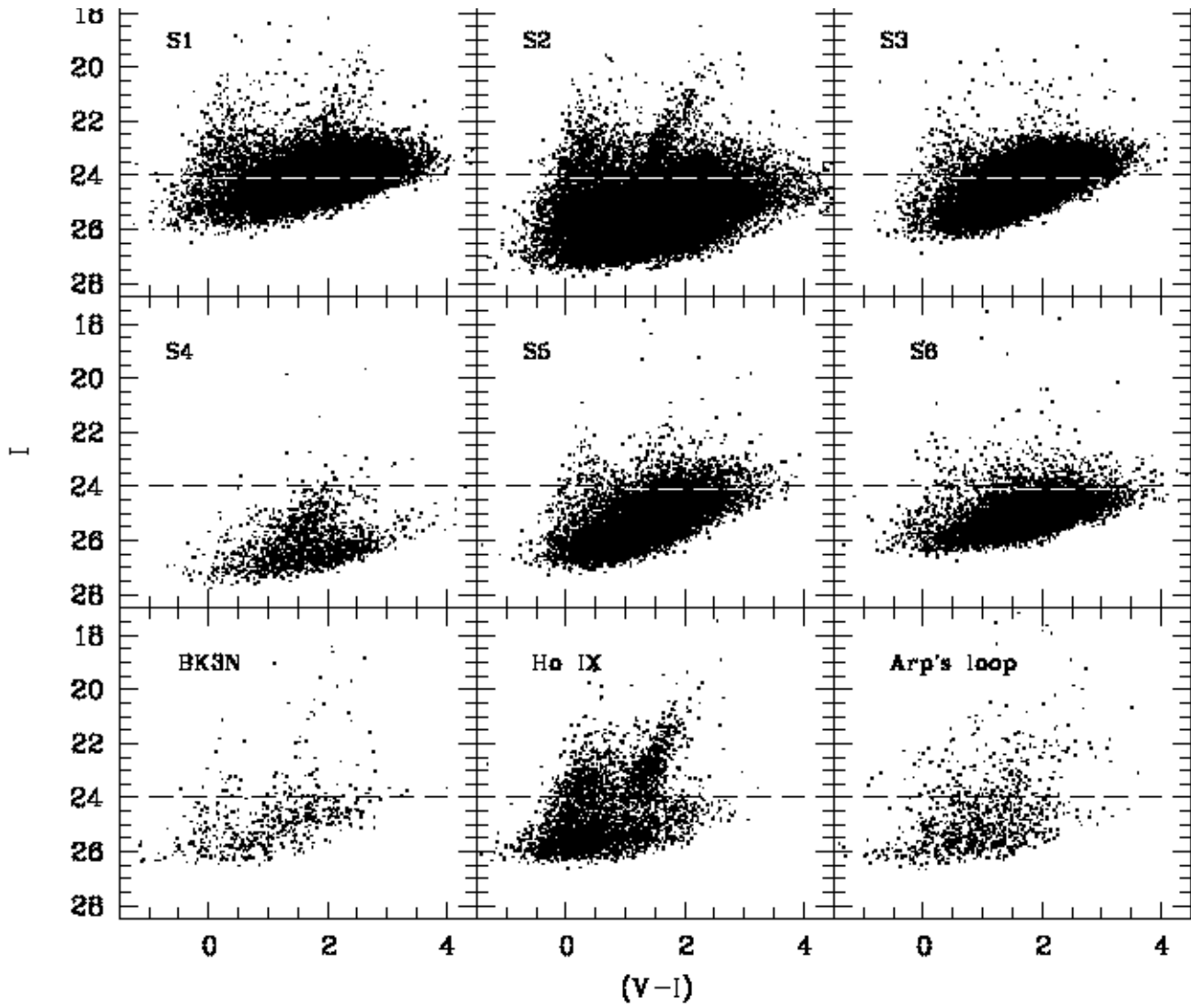


Fig. 4. $[(V - I), I]$ Color-Magnitude diagrams of different fields of M 81. The dashed line shows the position of the TRGB.

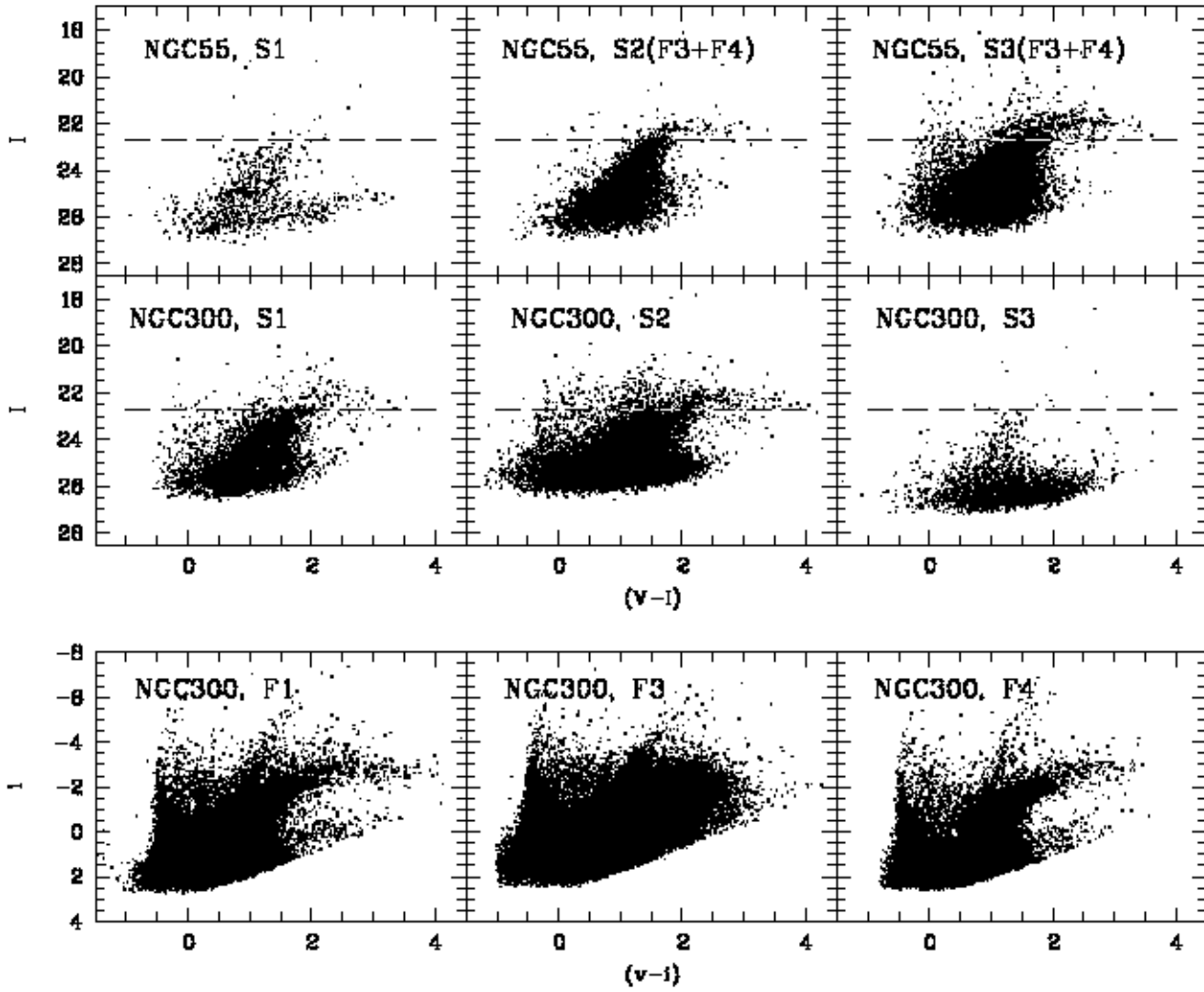


Fig. 5. $[(V-I), I]$ Color-Magnitude diagrams of different fields of NGC 55 and NGC 300. The dashed line shows the position of the TRGB. The ACS instrumental magnitude i and $(v-i)$ are presented without transformation to Kron-Cousins system.

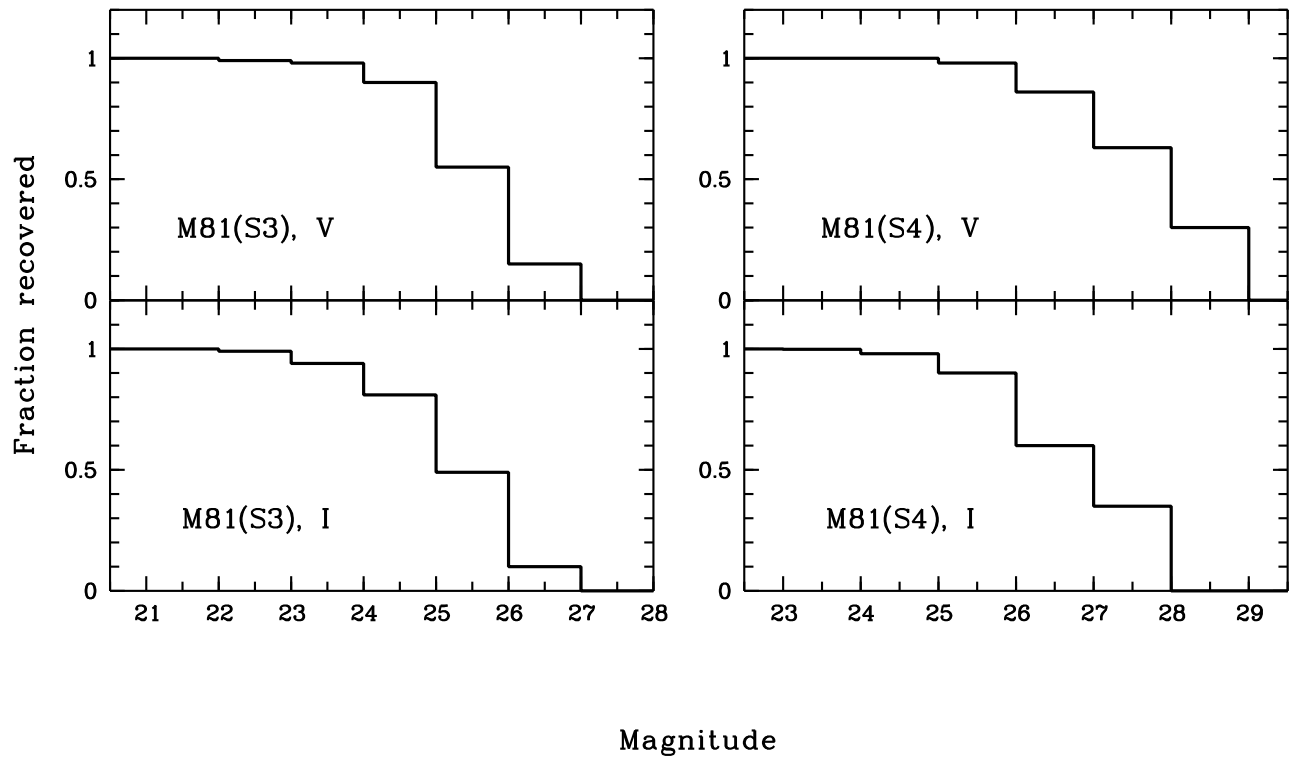


Fig. 6. Completeness levels of the WFPC2 photometry of the M 81 (S3 and S4 regions) based on artificial star test.

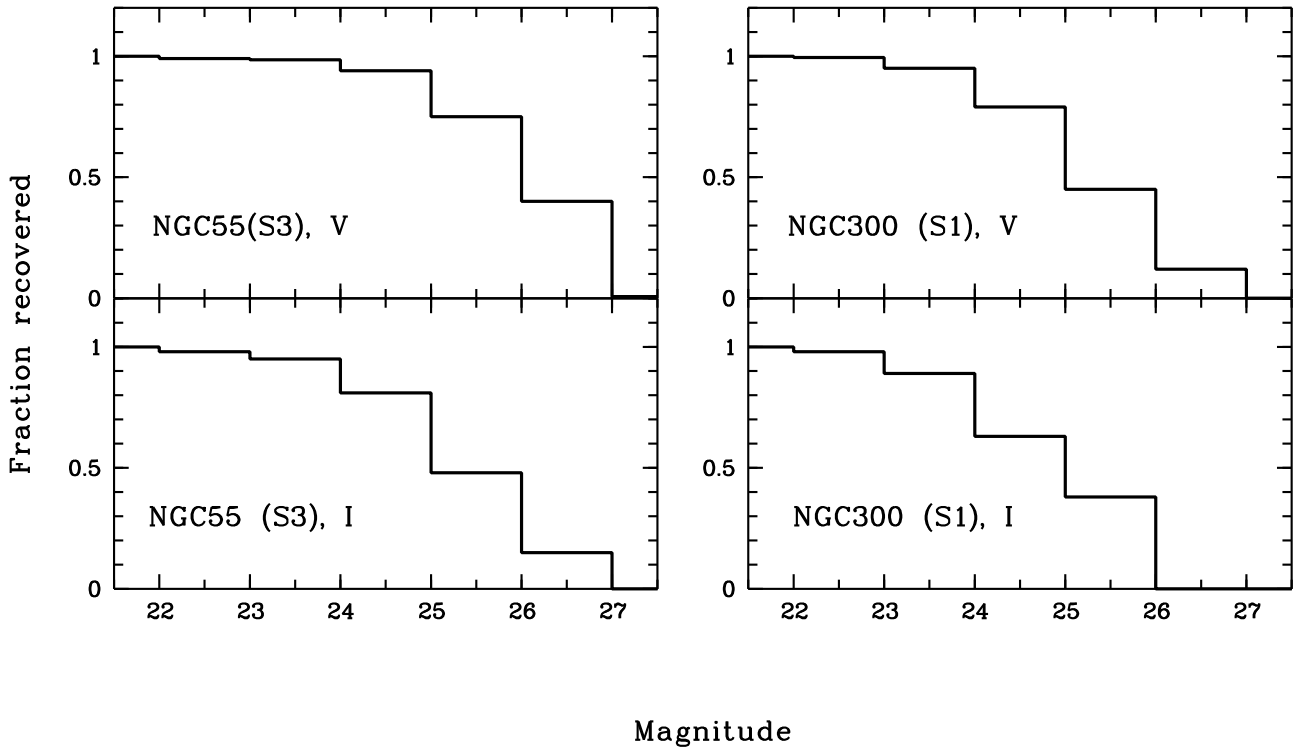


Fig. 7. Completeness levels for NGC 55 (Field S3) and NGC 300 (Field S1).

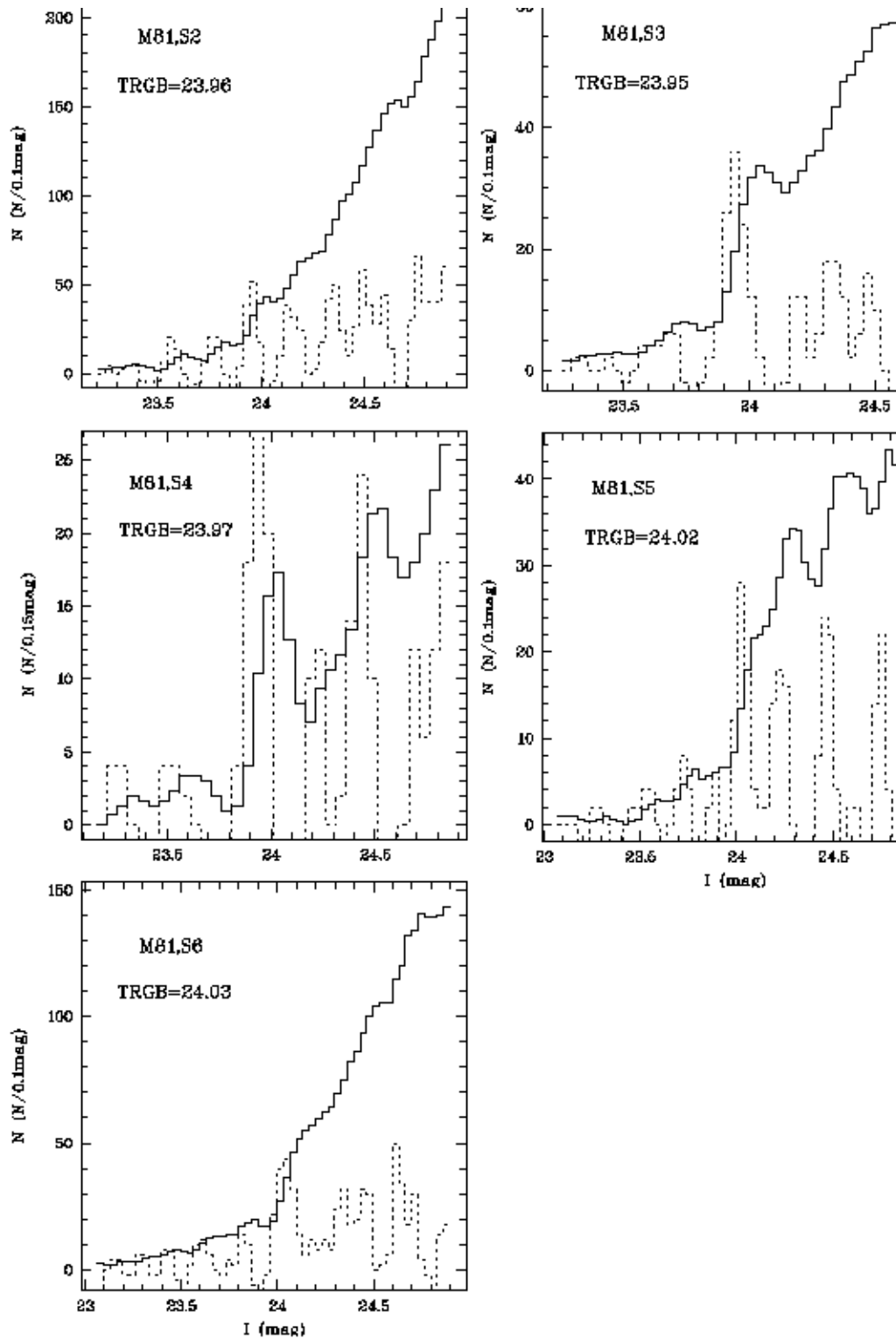


Fig. 1. Smoothed luminosity function LF (solid lines) and edge-detection filter output (dotted

Fig. 8. Smoothed luminosity function LF (solid lines) and edge-detection filter output (dotted lines) for different fields of M81. The position of the TRGB is identified with the peak in the output function.

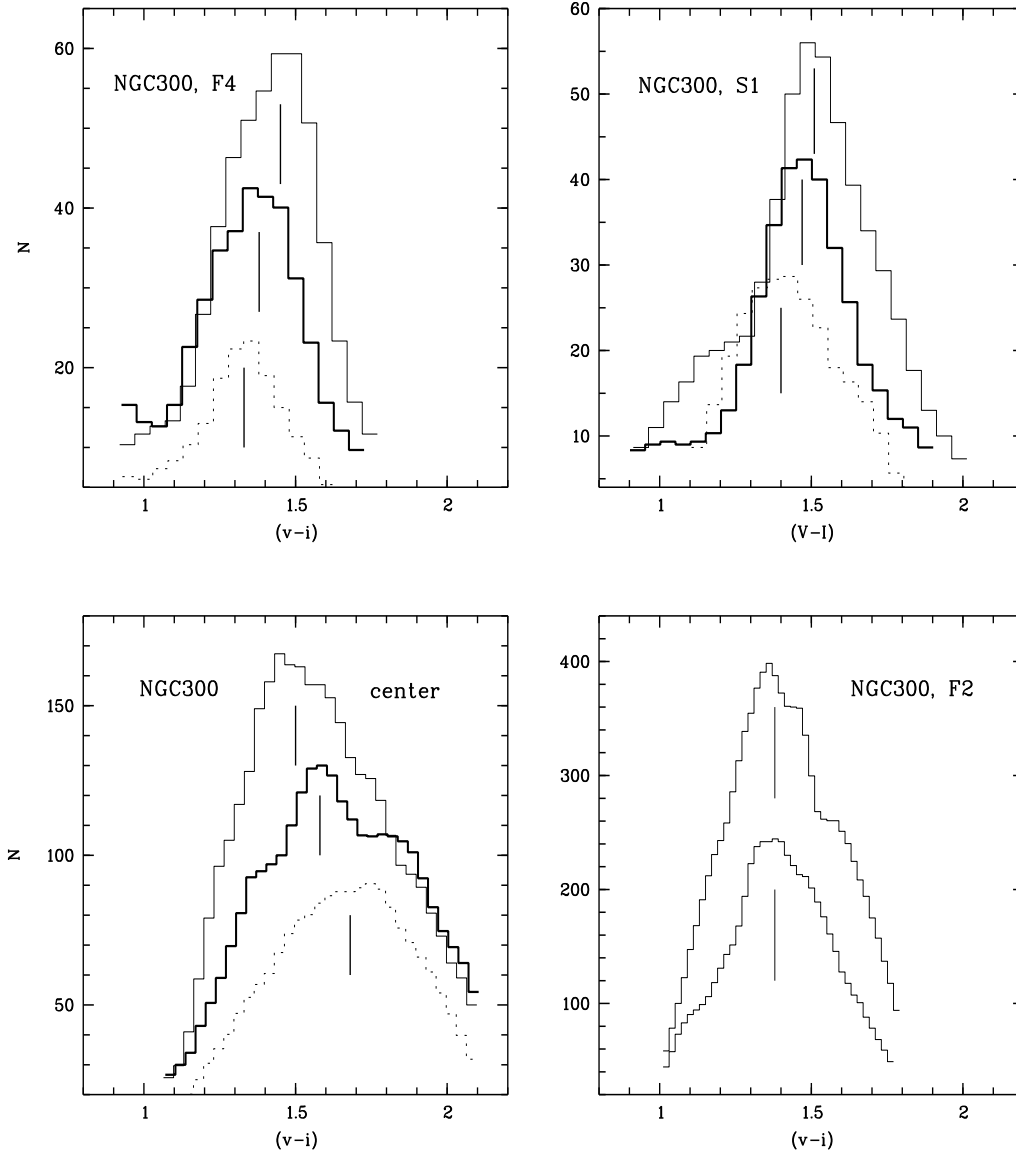


Fig. 9. $(V-I)$ and ACS-magnitude $(v-i)$ colour of the red giant branch of different fields NGC 300. Two fields (F4 and S1) are situated at the edge of galaxy and demonstrated decreasing colour along galactocentric radius. In the center field (F3) the colour of RGB decrease to the center of galaxy, due to effect of age and metallicity. In the field F2 that situated in the main body of galaxy, RGB colour do not change along radius. The solid line corresponds to more distant regions then the double width line or dash line.

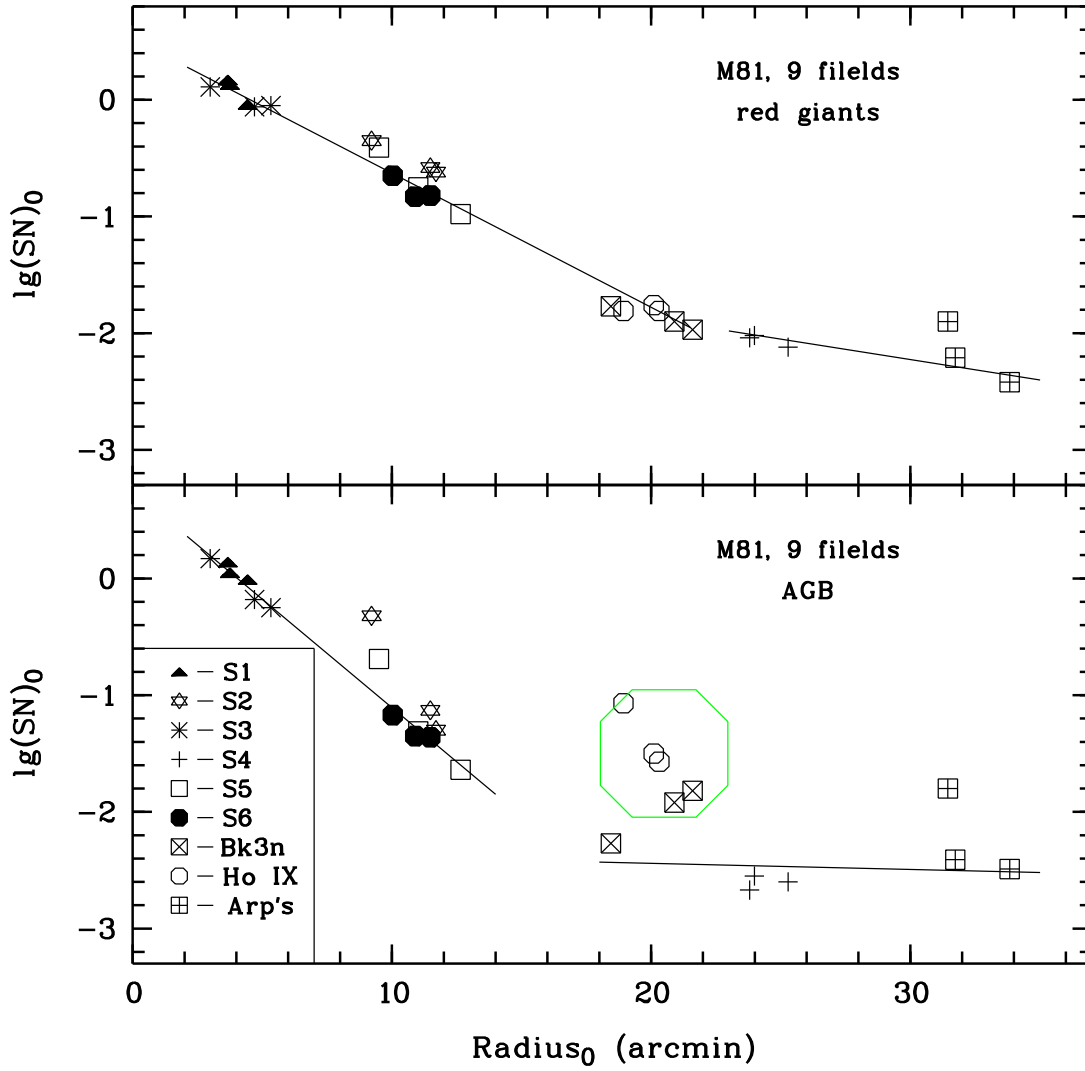


Fig. 10. The distribution of RGB (top) and AGB (bottom) stars along galactocentric radius of M 81. $Radius_0$ corrected for inclination of galaxy. $(SN)_0$ – surface number of stars after correction for incompleteness. The absence of data for $13' < Radius_0 < 18'$ is due to insufficient images in these regions. The deviation of some points from the average level of the stellar density is a result of summation of stars of disk (halo) of M 81 with the stars of dwarf galaxies (BK3N, Ho IX, Arp's ring).

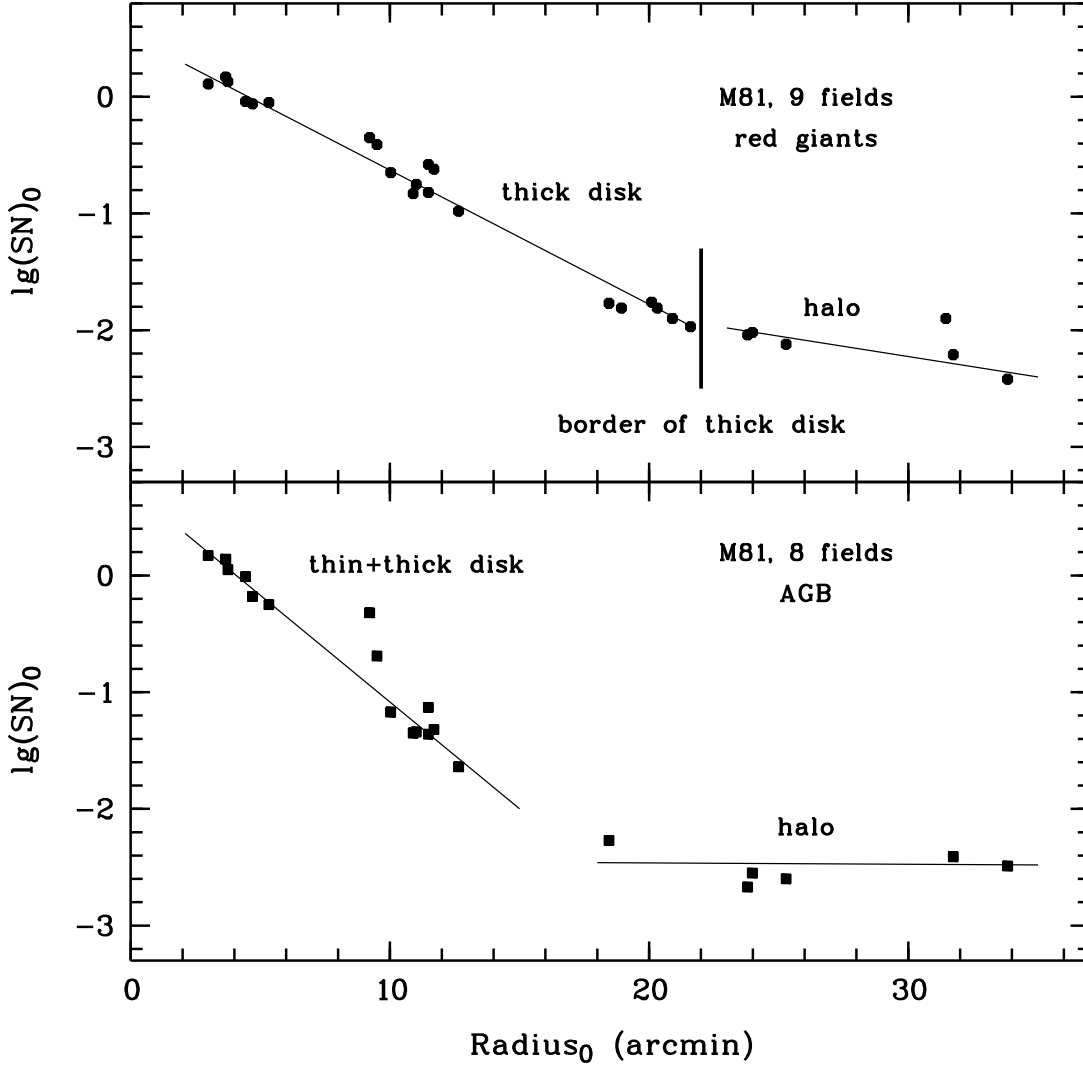


Fig. 11. The distribution of RGB (top) and AGB (bottom) stars along galactocentric radius of M 81. $Radius_0$ and $(SN)_0$ are the same as fig.10. The absence of data for $13' < Radius_0 < 18'$ is due to insufficient images in these regions. We do not consider the fields, where the influence the dwarf galaxy is too big. It is clearly seen, that the halo and the disk have different gradient of decreasing of stellar density. It is allow us to determine the border of thick disk.

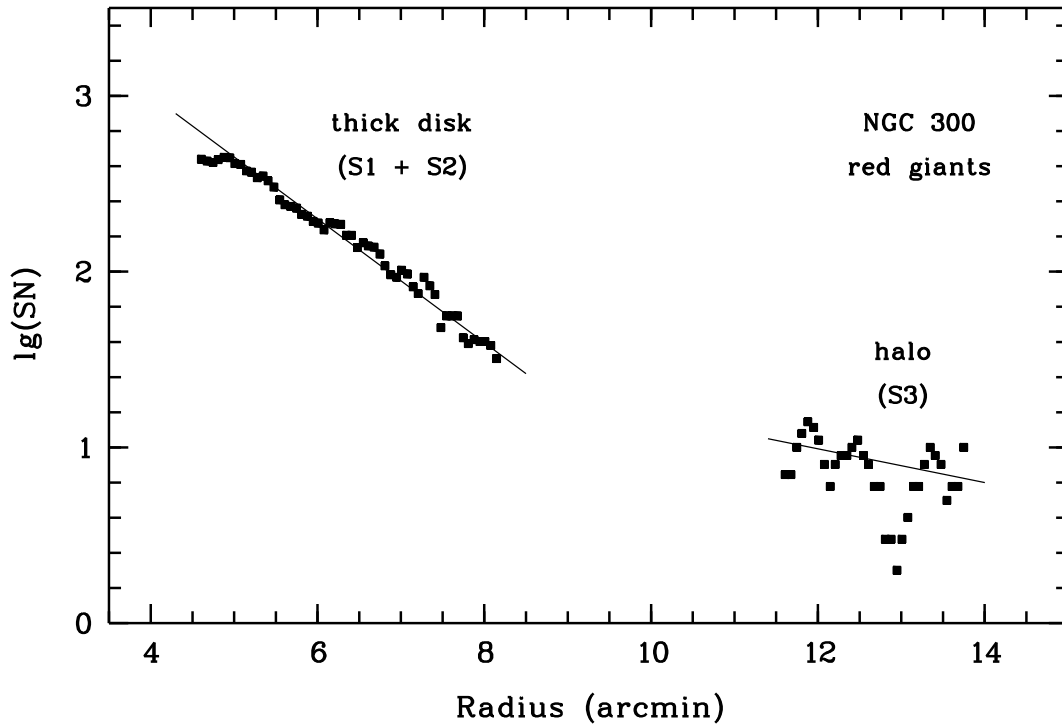


Fig. 12. The distribution of RGB stars along galactocentric radius. (SN) – surface number without any correction. Similar to the M 81 the stars of halo and the disk have different gradient of decreasing of stellar density.

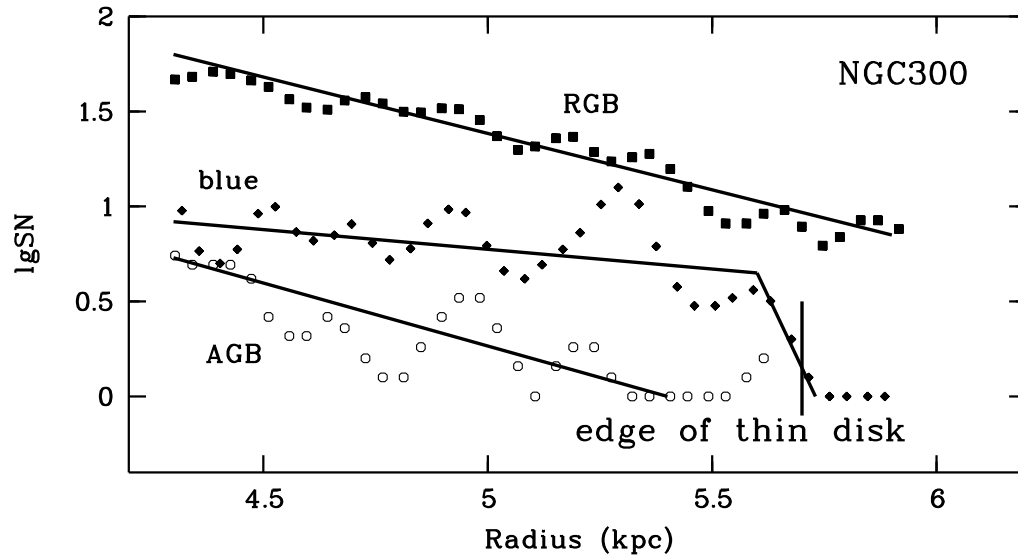


Fig. 13. The distribution of RGB, AGB and blue stars at the edge of thin disk in the S2 of NGC 300. (SN) is the same as fig. 12. The radius of the thin disk is 5.7 kpc. The number density of blue stars drops to zero at this radius, while the the red giants of the thick disk extend to larger distance.

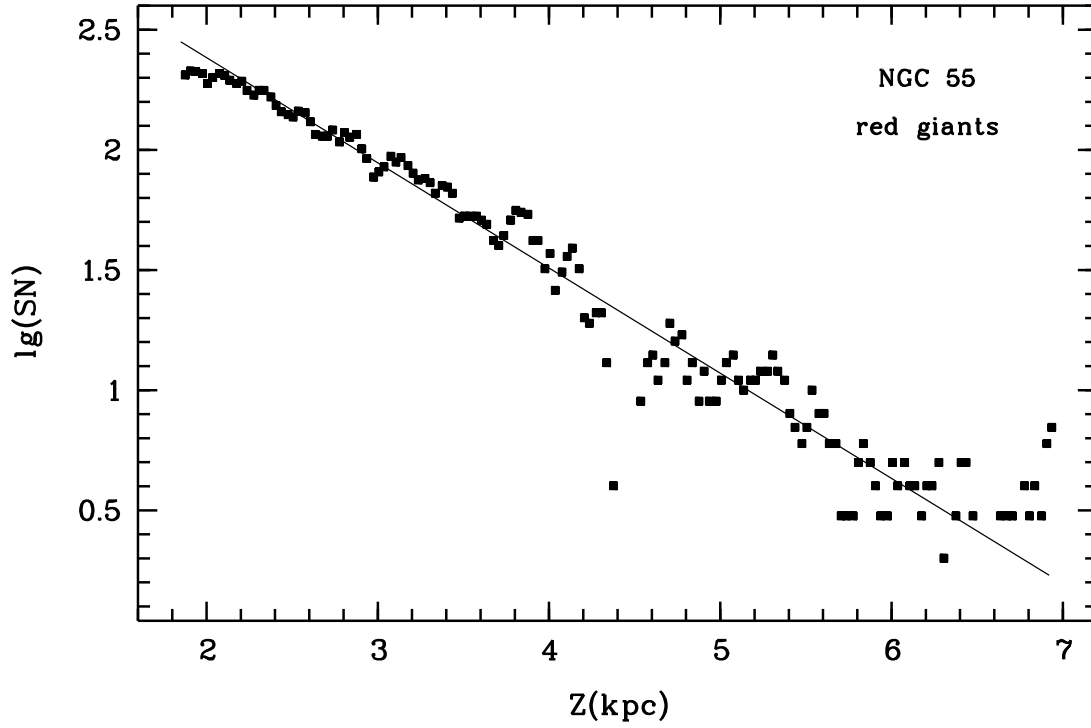


Fig. 14. The distribution of RGB stars in NGC 55 (S1, S2, S3 fields) perpendicular the galactic plane. There is the thick disk only. The trace of the halo is seen at a distance $Z > 6$ kpc.

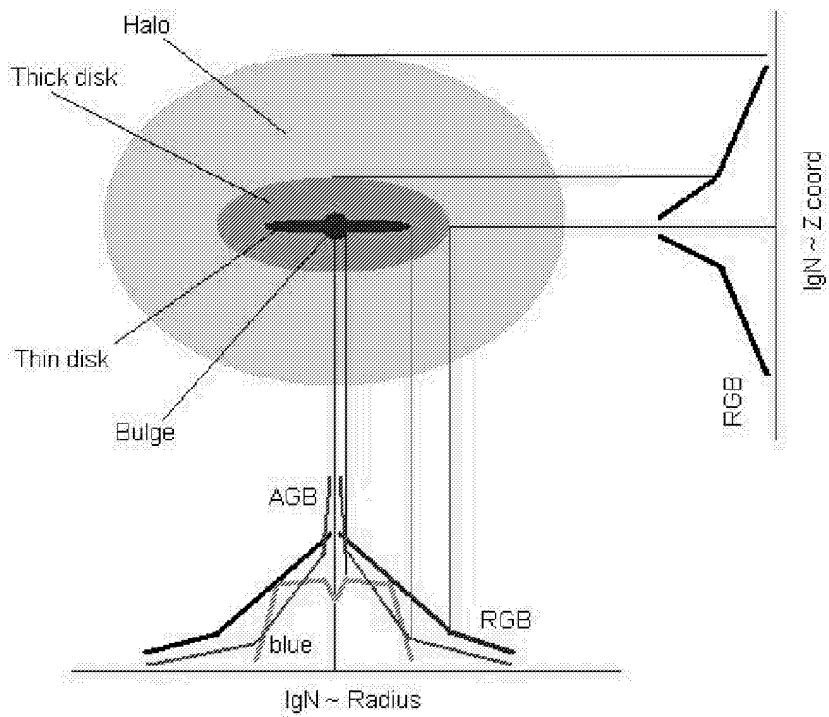


Fig. 15. Scheme of structures of the spiral galaxy that consistent with our investigations of stellar distribution. The thickness of thin disk is from Ma, 2002. The relative sizes of thick to thin disks are from our investigations of M81, NGC300 and M33 (Guilandre, 1998). The comparative size of halo of galaxies M81 and NGC300 are more extended then in this picture. Relative distribution of different types of stars along radius and Z coordinate displayed at bottom and right.